ELSEVIER

Image and Vision Computing 21 (2003) 473–482

www.elsevier.com/locate/imavis

Segmentation of multi-spectral images using the combined classifier approach

P. Paclík[a,*], R.P.W. Duin[a], G.M.P. van Kempen[b], R. Kohlus[b]

[a]Pattern Recognition Group, Faculty of Applied Science, Delft University of Technology, Lorentzweg 1, 2628 CJ Delft, The Netherlands
[b]Unilever Research Vlaardingen, 3130 AC Vlaardingen, The Netherlands

Received 18 May 2002; received in revised form 5 September 2002; accepted 23 January 2003

Abstract

Segmentation methods, combining spectral and spatial information, are essential for analysis of multi-spectral images. In this article, we propose such a method based on statistical pattern recognition algorithms and a combined classifier approach. A set of experiments is presented with multi-spectral images of detergent laundry powders acquired by imaging cross-sections with scanning electron microscopy using energy-dispersive X-ray microanalysis (SEM/EDX). The algorithm stability and the segmentation quality are investigated. The use of a priori information for the segmentation of images with similar spectral properties is studied as well. Finally, a comparison with probabilistic relaxation method for multi-spectral image segmentation is made.

Keywords: Multi-spectral imaging; Image segmentation; Classifier combination

1. Introduction

Multi-spectral quantitative analysis provides new possibilities for a qualitatively better description of natural processes or phenomena in many practical applications. Therefore, it has received a growing attention in fields like remote sensing and product inspection. The basic task performed by the majority of multi-spectral data analysis systems is image segmentation. A segmented multi-spectral image may serve for visualization purposes or for the further processing in order to describe, recognize, and interpret underlying physical modalities. In this paper, we present a method for the segmentation of multi-spectral images based on statistical pattern recognition methods. The paper, which is an extension of our conference article [14] describes the segmentation method developed for the structure analysis of multi-component, granular material.

Many methods have already been presented for the segmentation of gray-level or color images [4,6,15,16]. Generally, segmentation methods may be divided in four groups: edge-based, neighborhood-based, histogram-based, and cluster-based methods [12]. Edge-based methods search for discontinuities in the image while neighborhood-based employ the similarity between different image regions. The spatial domain of a processed image is used in both cases. Examples are edge-following and region growing algorithms. These methods cannot be effectively used for the multi-spectral image segmentation as their adaptation to the multi-dimensional data is not straightforward. On the contrary, histogram-based and cluster-based segmentation methods operate in the spectral domain. They consider individual image pixels as general data samples and assume correspondence between homogeneous image regions and clusters in the spectral domain.

The histogram-based algorithms perform mode seeking or multi-thresholding operation and relate the modes of a spectral histogram to homogeneous regions in the image [4,6]. It appears, however, that the increase of data dimensionality implies considerable memory requirements and the loss of precision. The cluster-based segmentation methods employ more general procedures to separate distinct structures in the spectral feature space. As an example, we can note multi-dimensional clustering methods like ISODATA or Fuzzy c-means clustering [9,10].

* Corresponding author. Address: Pattern Recognition Group, Delft University of Technology, P.O. Box 5046, Delft 2600 GA, The Netherlands. Tel.: +31-15-278-3191; fax: +31-15-278-6740.

E-mail addresses: pavel@ph.tn.tudelft.nl (P. Paclík), duin@ph.tn.tudelft.nl (R.P.W. Duin), geert-van.kempen@unilever.com (G.M.P. van Kempen), reinhard.kohlus@unilever.com (R. Kohlus).

0262-8856/03/$ - see front matter © 2003 Published by Elsevier Science B.V.
doi:10.1016/S0262-8856(03)00013-1

When designing a segmentation algorithm, one faces a fundamental dilemma—which data domain should be emphasized? It is a widely agreed fact, that robust algorithms for multi-spectral segmentation should employ both available domains—spectral and spatial. The issue of combining spectral and spatial information has been addressed by several authors. Spann and Wilson [17], for example, performed a quad-tree smoothing operation followed by feature clustering and boundary estimation. Their method requires spatially coherent image regions at different scales of the quad tree. Haralick and Shapiro [6] devised to use the combination of spatial region growing with the clustering procedure running in the spectral feature space. The method called 'spatial clustering' starts from the analysis of feature space histograms. The region growing procedure is performed by taking into account mutual pixel distances and estimated probabilities of class membership. Matas and Kittler [13] developed a method for the clustering of spatially related data called 'spatial and feature clustering'. This method is based on the graph-theoretical clustering approach. Segmentation method of Hauta-Kasari et al. starts by a quantization of the spectral domain by the self-organizing map [7]. The multi-spectral image is then labeled by the trained map. To analyze local spatial relationships, a co-occurrence matrix are then used for the training of a pattern classifier. The other technique, suitable for the segmentation of multi-spectral images is probabilistic relaxation [3,8]. For each pixel the probability of class membership is estimated given pixel features and its context. In the case of image segmentation is the pixel context usually represented by its local neighborhood.

The Algorithm 1, presented in this paper, treats the spatial and spectral domains separately. In both domains statistical classifiers are built and their outcomes are combined. The procedure is iterative and runs until a stable segmentation result is reached. The independent treatment of both data domains and a general way of combining the domain-specific information distinguishes the presented segmentation algorithm from other multi-spectral segmentation methods. Because the presented algorithm is constructed from general statistical pattern classifiers we refer to it as *classifier-based segmentation method* in the paper.

In Section 2, a formal description of the presented segmentation algorithm is given. Then, we discuss the application of the described method for the segmentation of multi-spectral images of multi-component granules. The algorithm stability and the issue of the segmentation quality are discussed. We also investigate the possibility to use a segmentation result as a priori information for the processing of similar images. The presented algorithm is an alternative approach to probabilistic relaxation. Therefore, we derive a simple relaxation model and compare the results of both segmentation methods in Section 3.5. Finally, we shortly discuss the presented method and give some ideas for future research.

2. The segmentation algorithm

The input of the segmentation algorithm is a multi-spectral image with D spectral bands. The algorithm output is the image labeling $\Lambda = \{\lambda_i\}$, $i = 1, \dots, N$, $\lambda_i \in \Omega$, where N denotes the number of image pixels and λ_i are pixel labels. Labels take values from a set of mutually exclusive classes $\Omega = \{\omega_1, \dots, \omega_C\}$.

The algorithm separates spectral and spatial information and works with a different dataset in each data domain. In the spectral domain, a dataset $\mathscr{D}_{\text{spec}}$ is built which contains a feature vector $\mathbf{x}_i \in \mathbb{R}^D$ for each image pixel. Individual features then correspond to spectral bands. The dataset therefore contains only the spectral information and all the spatial relationships are lost. In the spatial domain, a dataset $\mathscr{D}_{\text{spat}}$ is created containing a feature vector $\mathbf{x}'_i \in \mathbb{R}^2$ for each image pixel. In this case, features correspond to spatial pixel coordinates and the spectral information is omitted.

The first step of the segmentation algorithm is the construction of the initial labeling Λ_0 by allocation of each feature vector $\mathbf{x}_i$ into a class $\omega \in \Omega$. The initial labeling is performed by an unsupervised clustering algorithm on the spectral dataset $\mathscr{D}_{\text{spec}}$.

The second step of the segmentation algorithm is the iteration process using labeled spectral and spatial datasets to generate new labeling schemes. A classifier $\psi_{\text{spec}} : \mathbb{R}^D \to \Omega$ is trained on the spectral dataset $\mathscr{D}_{\text{spec}}$. Class conditional a posteriori probabilities $\hat{P}_{\text{spec}}(\omega_C|\mathbf{x}_i)$, $c = 1, \dots C$, are then estimated for all data samples using the trained spectral classifier. In similar way, a spatial classifier $\boldsymbol{\psi}_{\textbf{spat}} : \mathbb{R}^D \to \Omega$ is trained on the dataset $\mathscr{D}_{\text{spat}}$. For each data sample, class conditional a posteriori probabilities $\hat{P}_{\text{spat}}(\omega_C|\mathbf{x}'_i)$, $c = 1, \dots, C$ are estimated.

Algorithm 1. Segmentation of multi-spectral image

input: multi-spectral image I, number of classes C
initial labeling: find initial labeling Λ_0 by clustering algorithm
iter = 0
repeat
· iter = iter + 1
· create $\mathscr{D}_{\text{spec}}$ (spectral data and labels $\Lambda_{\text{iter}-1}$)
· train spectral classifier ψ_{spec} on dataset $\mathscr{D}_{\text{spec}}$
· estimate $\hat{P}_{\text{spec}}$ running ψ_{spec} on $\mathscr{D}_{\text{spec}}$
· create $\mathscr{D}_{\text{spat}}$ (pixel positions and labels $\Lambda_{\text{iter}-1}$)
· train spatial classifier ψ_{spat} on dataset $\mathscr{D}_{\text{spat}}$
· estimate $\hat{P}_{\text{spat}}$ using ψ_{spat} on $\mathscr{D}_{\text{spat}}$
· get $\hat{P}_{\text{comb}}$ by combining $\hat{P}_{\text{spec}}$ and $\hat{P}_{\text{spat}}$ together
· generate new labels Λ_{iter} from $\hat{P}_{\text{comb}}$
until diff ($\Lambda_{\text{iter}-1}$, Λ_{iter})
output: segmented image Λ_{iter}

So far, two separate datasets have been used in the segmentation process: $\mathscr{D}_{\text{spec}}$ in the spectral and $\mathscr{D}_{\text{spat}}$ in the spatial domain. Two sets of a posteriori probabilities were therefore computed in these domains for each individual pixel. The a posteriori probabilities are then combined by a classifier combination method. Different combination strategies may be used such as the maximum, product, or mean rule. We have chosen the product rule because we assume statistical independence of both combined representations (spectral and spatial) [11]:

$$\hat{P}_{\text{comb}}(\omega|\mathbf{x}_i) = \frac{\hat{P}_{\text{spec}}(\omega|\mathbf{x}_i)\hat{P}_{\text{spat}}(\omega|\mathbf{x}'_i)}{\sum_{c=1}^{C}\hat{P}_{\text{spec}}(\omega_C|\mathbf{x}_i)\hat{P}_{\text{spat}}(\omega_C|\mathbf{x}'_i)} \quad \forall i,\ i = 1,\dots,N \tag{1}$$

The a posteriori probability $\hat{P}_{\text{comb}}(\omega_c|\mathbf{x}_i)$ determines a new labeling Λ_1 :

$$\lambda_i = \arg\max_C \{\hat{P}_{\text{comb}}(\omega_C|\mathbf{x}_i)\},\ \ \Lambda_1 = \{\lambda_i\} \quad \forall i,\ i = 1,\dots,N \tag{2}$$

The labeling Λ_1 is then used to generate the spectral and spatial datasets $\mathscr{D}_{\text{spec}}$ and $\mathscr{D}_{\text{spat}}$, again. The segmentation algorithm, presented in Fig. 1, is therefore an iterative procedure starting from the initial labeling estimate Λ_0. In the loop, results of spectral and spatial classifies are combined together and new labeling schemes are developed until a stable segmentation is reached.

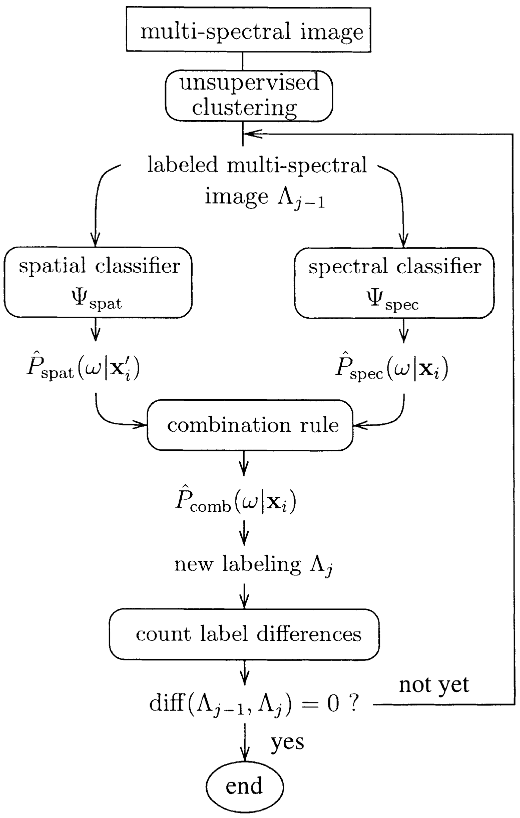

Fig. 1. The segmentation algorithm.

Let us define the number of label changes between two sets of labels Λ_a and Λ_b $\text{diff}(\Lambda_a, \Lambda_b)$ as

$$\text{diff}(\Lambda_a, \Lambda_b) = \sum_{i=1}^{N} \mathscr{I}(\Lambda_a(i), \Lambda_b(i)), \tag{3}$$

where $\mathscr{I}$ is the indicator function:

$$\mathscr{I}(\lambda_m, \lambda_n) = \begin{cases} 1 & \text{if } \lambda_m \neq \lambda_n \\ 0 & \text{otherwise.} \end{cases} \tag{4}$$

The labeling scheme $\Lambda_j, j \geq 1$ is then stable if $\text{diff}(\Lambda_{j-1}, \Lambda_j) = 0$.

During the segmentation, different algorithms may be used to generate the initial labeling and to build the spectral and spatial domain classifiers. The final segmentation result depends on the actual dataset and is also influenced by the performance of spectral and spatial classifiers. It is difficult to make any general statements about the segmentation stability. The actual behavior of the segmentation algorithm and the issue of the observed segmentation stability is discussed further in Section 3.

3. Experiments with the classifier-based segmentation method

This section describes several experiments with the presented segmentation algorithm on a set of multi-spectral images of laundry detergents. First, we describe the application, dataset and the evaluation procedure. Then, we explain the actual setup of the classifier-based segmentation. In order to evaluate the performance of the presented method, a comparable probabilistic relaxation model is derived in Section 3.4. Eventually, the experimental results of both approaches are presented and discussed in Section 3.5.

3.1. Application of interest and experimental dataset

The presented classifier-based segmentation algorithm has been developed in order to segment multi-spectral images of multi-component granules acquired by scanning electron microscopy (SEM). The spatial arrangement of the three constituent clusters, which are solids, actives and porosity, determines largely the properties of the product, here the detergent powder. Structure analysis is therefore of key importance in the assembly and the optimization process of such material. A crucial intermediate step is the segmentation of images depicting the granule structure in the three mentioned clusters.

The spatial information about the structural arrangement of granule cross-sections is obtained by SEM. The spectral information, necessary to distinguish different underlying modalities, is acquired by the method of energy-dispersive X-ray microanalysis (EDX).

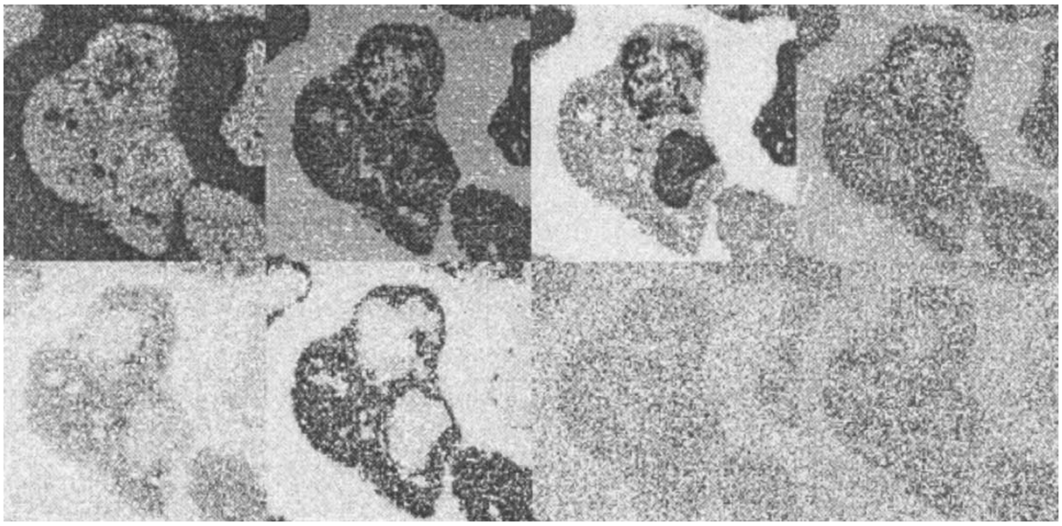

Fig. 2. Multi-spectral image with eight bands acquired by SEM/EDX method.

The SEM/EDX method generates the multi-spectral image by delivering the information about chemical elements for each image pixel [5]. The experimental dataset consists of five multi-spectral images of laundry detergent powders. All the images render similar material using eight spectral bands. The size of the images is 128×128 pixels. An examples of a multi-spectral image acquired by SEM/EDX method is shown in Fig. 2.

3.2. Evaluation of segmentation algorithms

The image segmentation task, introduced in Section 2, is inherently a clustering problem because the true class labels are not known. However, in order to evaluate performance of segmentation algorithms, some form of 'ground-truth' labeling is necessary. We decided to use images, segmented by application experts, as a substitute of the true image labeling.

The experts, in fact, hand-painted the label images taking into account information in all spectral bands. The outcome of this time-consuming process naturally depends on the expert's experience, insight, and subjective interpretation of multi-spectral data. Different experts, therefore, produce slightly different hand-labeled images which is illustrated in Fig. 3. Variability of hand-labeling images, created by different experts, usually does not exceed 8% of label differences.

The only ultimate criterion to measure the quality of a clustering result is the eventual judgment of a human expert which is, unfortunately, hard to quantify. Therefore, we use also a number of label differences to measure the closeness between segmentation result and a hand-labeling.

3.3. Classifier-based segmentation

In all experiments, the following setup was used: the initial image labeling Λ_0 was derived by the k-means clustering of a randomly generated dataset with 500 pixels. The initial labeling was then used by the segmentation algorithm separately in both data domains (see Fig. 1). In the spectral domain, the nearest mean classifier was used. The outcome of a classifier was converted into a posteriori probability estimate [2]. In the spatial domain, we have used a Parzen classifier with a Gaussian kernel which could easily be implemented using a convolution. If not mentioned explicitly, the smoothing parameter σ of the Parzen classifier was set to $\sigma = 1.0$ pixel. The presented segmentation algorithm treats the number of classes as an input parameter. The application experts suggested to work with three classes because of the three main components of a detergent powder: solids, actives, and pores.

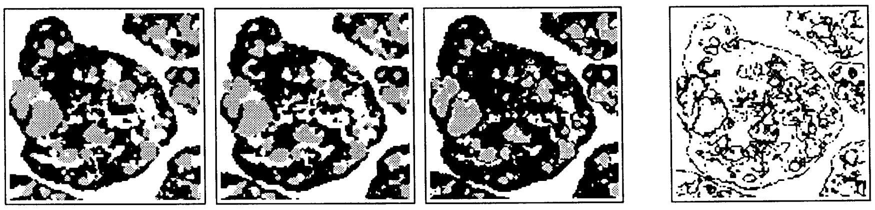

Fig. 3. Three hand-labeled images produced by different experts for the same multi-spectral dataset. The rightmost image highlights all differently labeled pixels.

3.4. Probabilistic relaxation

Probabilistic relaxation is a general approach to label a group of objects using their features and context information [1,18]. When applied in the field of image segmentation it provides us with another way to combine the spectral and spatial domain information. In this section we derive a simple probabilistic relaxation model which is used later for the sake of comparison.

The Probabilistic relaxation is an iterative procedure assigning class labels to individual pixels on the basis of estimated class conditional a posteriori probabilities. The a posteriori probability of class membership $P(\omega|\mathbf{x}_i, C_i)$, given spectral data $\mathbf{x}_i$, of pixel i and its context C_i, may be expressed as:

$$P(\omega|\mathbf{x}_i, C_i) = \frac{P(\omega, \mathbf{x}_i, C_i)}{\sum_{c=1}^{C} P(\omega_C, \mathbf{x}_i, C_i)} \tag{5}$$

Assuming the statistical independence between pixel features $\mathbf{x}_i$ and its context C_i, we can express the probability $P(\omega, \mathbf{x}_i, C_i)$ as:

$$\begin{aligned} P(\omega, \mathbf{x}_i, C_i) &= P(\mathbf{x}_i, C_i|\omega)P(\omega) = P(\mathbf{x}_i|\omega)P(C_i|\omega)P(\omega) \\ &= P(\omega|\mathbf{x}_i)P(C_i|\omega)P(\mathbf{x}_i). \end{aligned} \tag{6}$$

By substituting the result into the Eq. (5) we obtain:

$$P(\omega|\mathbf{x}_i, C_i) = \frac{P(\omega|\mathbf{x}_i)P(C_i|\omega)}{\sum_{c=1}^{C} P(\omega_c|\mathbf{x}_i)P(C_i|\omega_c)}. \tag{7}$$

The probability $P(\omega|\mathbf{x}_i)$ represents the spectral properties of given pixel. The probability $P(C_i|\omega)$ reflects, on the other hand, conditions in the pixel context. We model the context as local pixel neighborhood and assume the statistical independence between individual pixel neighbors:

$$P(\omega|\mathbf{x}_i, C_i) = \frac{P(\omega|\mathbf{x}_i) \prod_{j \in C_i} P(\mathbf{x}_j|\omega)}{\sum_{c=1}^{C} P(\omega_c|\mathbf{x}_i) \prod_{j \in C_i} P(\mathbf{x}_j|\omega_c)} \tag{8}$$

Actual pixel labels are then assigned using estimate of the a posteriori probability $\hat{P}(\omega|\mathbf{x}_i, C_i)$:

$$\forall i,\ i = 1,\ldots,N,\ \lambda_i = \arg\max_c \{\hat{P}(\omega_C|\mathbf{x}_i)\}.\ \Lambda = \{\lambda_i\}. \tag{9}$$

The segmentation based on the relaxation method is an iterative procedure started form an initial labeling. In each iteration, the posterior 8 is recomputed, based on an updated labeling of a training set. The algorithm is terminated when the segmentation becomes stable—when no single pixel changes its label between iterations. The class conditional probability $P(\mathbf{x}_i|\omega)$ is modeled by a Gaussian distribution with an equal covariance matrix for all classes. We have chosen this model because of its similarity to the nearest mean classifier used in the spectral domain of the classifier-based segmentation algorithm.

Let us now explain the differences between the probabilistic relaxation and the presented classifier-based segmentation algorithm. In the probabilistic relaxation framework, spectral information and the pixel context information are used in the Bayesian scheme. The relaxation model, used in the experiments, works on the spectral information in the local pixel neighborhood. It assumes mutual independence of pixel spectral properties and its context which implies the use of product combination rule. On the contrary, the classifier-based segmentation algorithm treats the spectral and spatial domains separately and combines attained results in a general way be combining corresponding classifiers.

3.5. Experimental results

3.5.1. Classifier-based segmentation

Fig. 4 illustrates the process of classifier-based segmentation. The first image in each row represents the initial labeling, generated by k-means clustering. This already captures much of the underlying data structure but also contains a lot of 'noise'. By noise in the segmentation result we mean inhomogeneous labeling. The noise is introduced by the clustering algorithm operating only in the spectral domain. Outcomes of the first two algorithm iterations and the stable segmentation result are given, subsequently. Finally, the hand-labeled image is presented.

Pixels changing their labels between algorithm iterations are shown for the first image. The evolution of the number of label changes for all five images is given in Fig. 5. The number of label changes decreases in all cases quickly to zero. The zero number of label differences corresponds to the stable segmentation result. It follows from our experiments with different classifiers and combination rules that the number of label changes decreases in a similar manner which leads to a stable segmentation.

3.5.2. The use of a priori information in segmentation

When a number of similar multi-spectral images is analyzed at the same time the segmentation algorithm may benefit from the use of a priori information. We have investigated the possibility of using a trained spectral classifier, which is a byproduct of the classifier-based segmentation, for the generation of initial labeling on a set of images with similar spectral properties.

In the experiment we use two multi-spectral images A and B. In the first step, the segmentation algorithm is run on both images generating label images Λ^{A} and Λ^{B}, respectively. Then, the image B is segmented again but this time using the initial labels provided by the trained classifier $\Psi^{\mathrm{A}}_{\mathrm{spec}}$. The result is the labeling $\Lambda^{B|A}$. Similarly, the image A is processed starting from the classifier $\Psi^{\mathrm{B}}_{\mathrm{spec}}$ producing

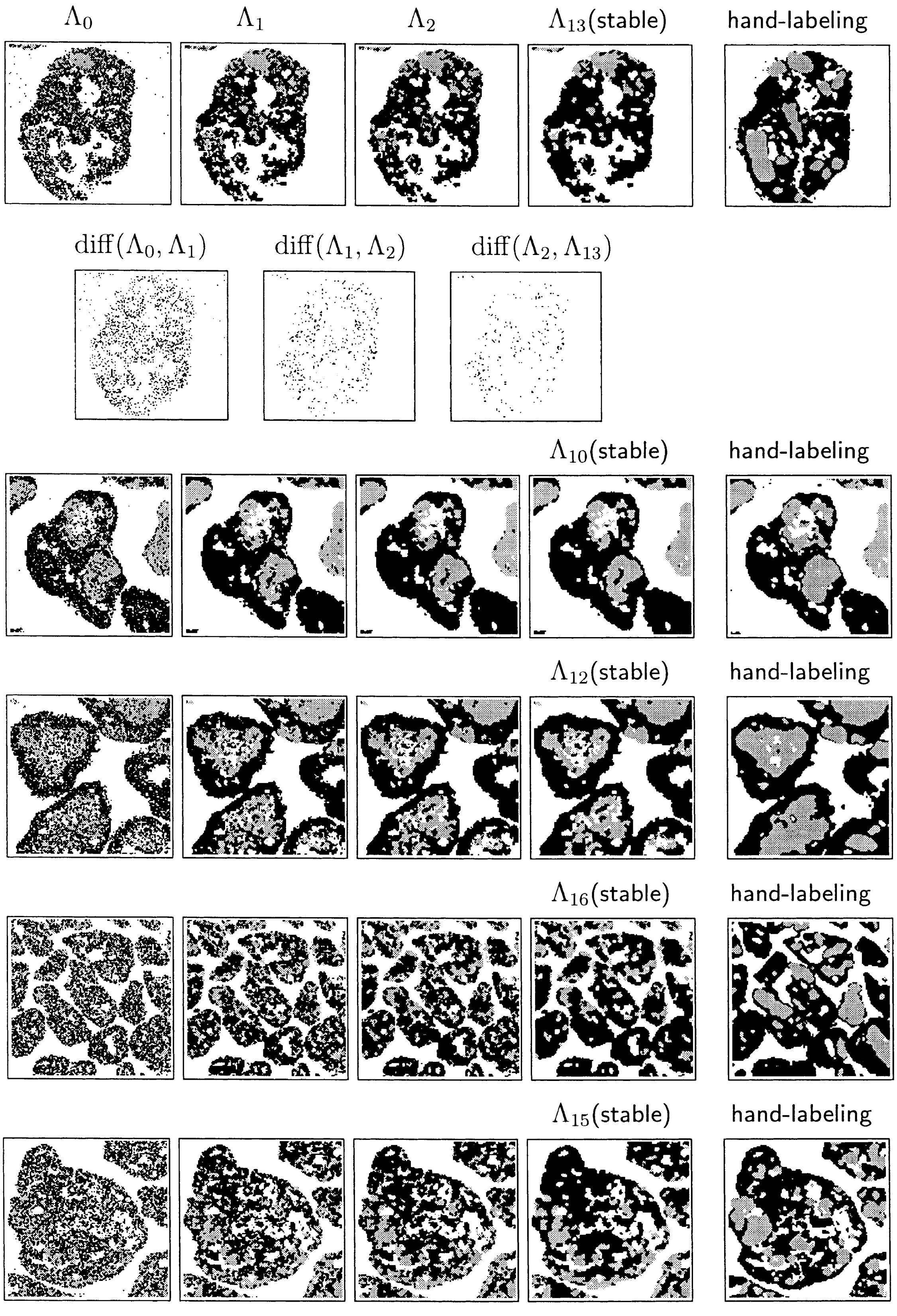

Fig. 4. Segmentation results for five multi-spectral images. For each image, initial labeling Λ_0 is given together with results of first two iterations (label images Λ_1, Λ_2). Stable segmentations and hand-labeled images are then presented. For the first image, the differences between label images are also shown (diff(Λ_0, Λ_1), diff(Λ_1, Λ_2), and diff(Λ_2, Λ_{13})).

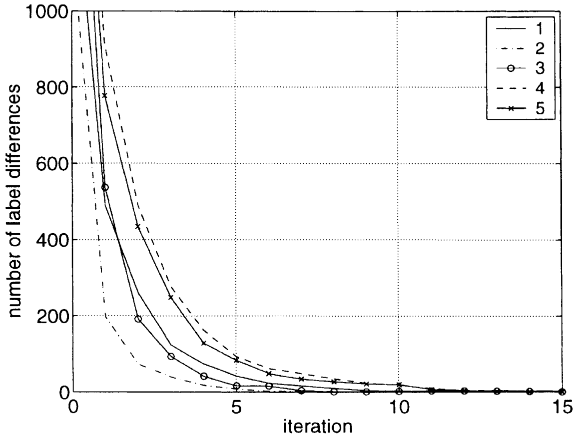

Fig. 5. Number of label changes between subsequent segmentation results during the iterative process (five different multi-spectral images 128 × 128 pixels).

the labeling $\Lambda^{A|B}$. Schematic overview of this cross-segmentation experiment is given in Fig. 6.

Now, the results obtained by the complete segmentation algorithm (e.g. Λ^{A}) may be compared with labeling based on the a priori spectral information ($\Lambda^{A|B}$). It follows from our experiments, that segmentation quality expressed by the label mismatch with hand-labeling is not significantly different for complete and a priori information-based segmentations. Nevertheless, the segmentation using the a priori information is considerably faster than the complete segmentation (see results in Table 1). While the spectral data clustering takes 30 s on average, the initial labeling by the trained spectral classifier takes just 0.8 s. These times were measured on a Pentium III 866 MHz processor. The execution time of initialization by the trained spectral classifier does not differ for different images as the same operation with the same amount of the data is performed each time. On the other hand, the speed of the initial clustering depends on the processed dataset and is influenced by the random initialization.

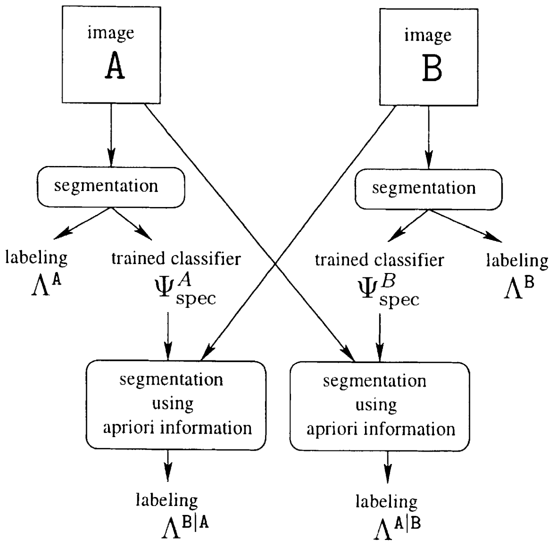

Fig. 6. Cross-segmentation of two images with a priori information.

Table 1
Speed measurements (in seconds) for both segmentation methods on Pentium III 866 MHz processor. Numbers are averages and standard deviations for 40 experiments

	Complete seg.	Using a priori inf.	Prob. relaxation
Initial labeling [sec]	30.1 ($\sigma = 1.8$)	0.8	30.1 ($\sigma = 1.8$)
Time of one iteration [sec]	2.7 ($\sigma = 0.8$)	2.7 ($\sigma = 0.8$)	7.0 ($\sigma = 1.4$)
Number of iterations [1]	16.5 ($\sigma = 0.9$)	16.5 ($\sigma = 0.9$)	18.1 ($\sigma = 1.4$)

3.5.3. Comparison with probabilistic relaxation

The comparison of segmentation results obtained by the presented classifier-based algorithm and using the probabilistic relaxation model, derived in Section 3.4, is given in Fig. 7. The same initial labeling, generated by the *k*-means clustering, was used for both algorithms. Segmentations were stopped automatically reaching the stable labeling. For each image, label mismatch with respect to the hand-labeling is given. Based on this criterion, the presented algorithm outperforms probabilistic relaxation in four from five cases. Application experts were also asked to judge the outcome. The results of the classifier-based algorithm were considered satisfactory for the structural analysis of laundry detergents. In some cases, the results appeared to reveal more detailed structures than the over-smoothed images painted by human.

We have also studied the behavior of both segmentation methods for variables sizes of local neighborhood. The classifier-based algorithm uses Parzen classifier in the spatial domain. Its local properties are determined by the smoothing parameter σ. Probabilistic relaxation approach works with the local pixel neighborhood. To compare the results of both methods, smoothing σ of the Parzen classifier was chosen to cover the neighborhood window of the relaxation algorithm with probability 0.95. Both methods were started from identical initial labeling. Segmentation results are presented in Fig. 8. Both methods reduce the noise of the initial labeling and deliver homogeneous results. The results of the probabilistic relaxation contain thin artifacts surrounding image regions. Their width depends on the size of local pixel neighborhood. It follows from experience of application experts, that these additional artifacts do not corresponds to the evidence in the analyzed images.

In the last experiment, we investigated stability of the segmentation result regarding different initializations by clustering. Complete cross-segmentation experiment (see Fig. 6) was performed 30 times for each segmentation method. Therefore, we have obtained four sets of segmentation results for each method (two complete segmentations and two a priori-information

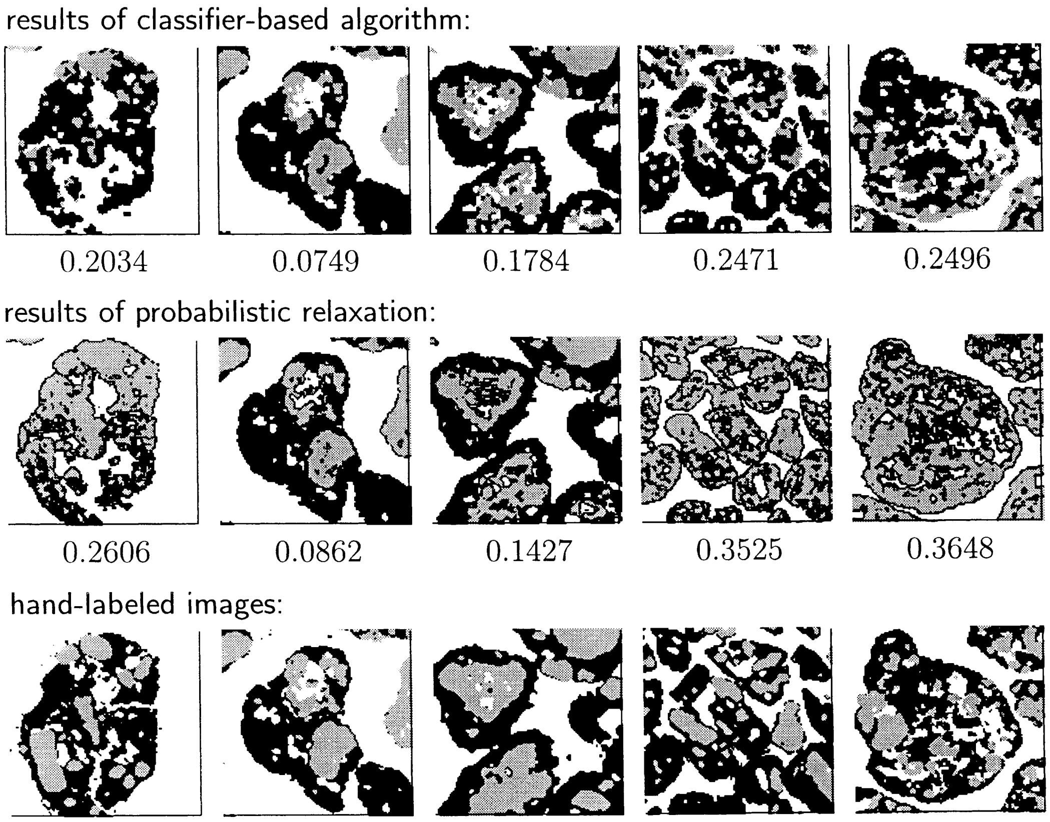

Fig. 7. Segmentation results obtained from combined classifier method (upper row) and probabilistic relaxation (middle row). Numbers below images are label mismatches with respect to hand-labeled images (lower row).

based segmentations). We have estimated the probability that a particular pixel will be labeled differently than in the 'most common' way. This probability estimate was computed for each pixel from number of occurrences of the most frequent label and a number of 'other' labelings. Results are given in Table 2 as the average number of changing their labels. Fig. 9 then shows the pixels with non-zero probability of a label change for the worst case in our experiment (complete segmentation of image B). It can be seen, that larger variations exist between the segmentation results of the probabilistic relaxation method than between the results of the classifier-based algorithm. We have also found out that each set of segmentation results contains several completely identical solutions (label images).

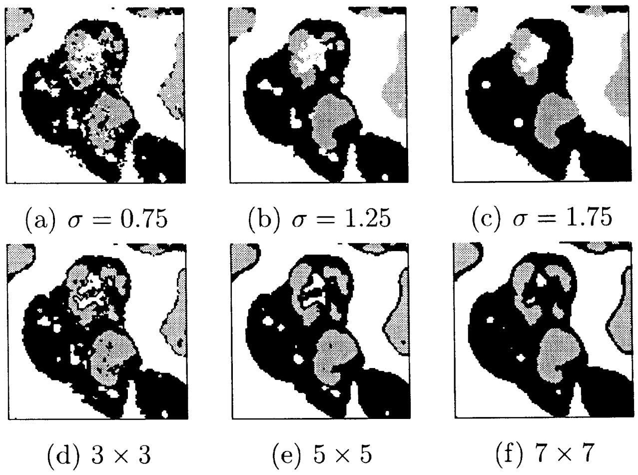

Fig. 8. Segmentation results obtained by the classifier-based method (upper images) and probabilistic relaxation (lower images). Value of smoothing or local neighborhood size is given for each image.

Table 2
Average number of image pixels ($\bar{\mu}$) changing their labels in a set of segmentation results for classifier-based segmentation and for probabilistic relaxation. Each table row represents a set of 30 randomly initialized segmentations (experiment schema in Fig. 6). Total number of image pixels is 16,384

Segmentation	Classifier-based segmentation	Probabilistic relaxation
Image A, complete segmentation	1.36	503.31
Image A, using a priori inf. form B	0.0	616.55
Image B, complete segmentaion	42.5	635.24
Image B, using a priori inf. from A	1.15	499.21

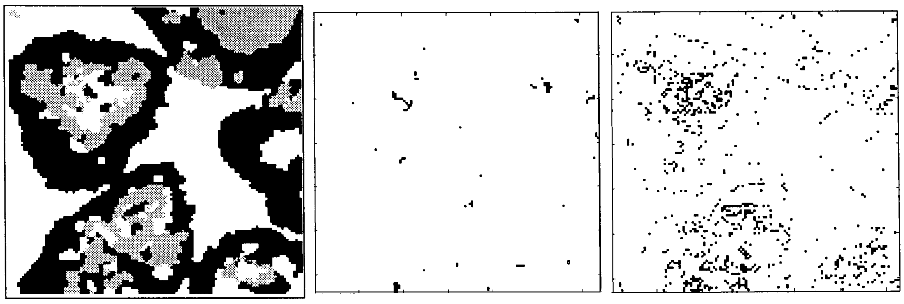

Fig. 9. Segmentation stability. The left image is a segmentation result. Binary images show pixels with a non-zero probability of label change in a set of segmentations started by different random initialization of the initial labeling algorithm. The image in the middle corresponds to the classifier-based segmentation and the rightmost image to the probabilistic relaxation.

4. Conclusion

A new algorithm for the segmentation of multi-spectral image has been presented. It is based on statistical pattern recognition algorithms and combines spectral and spatial domain information by a general approach of classifier combination. In the first step of the algorithm, initial image labeling is generated using the unsupervised clustering method. Then, two different datasets are constructed in both available data domains (spectral and spatial) and a statistical classifier is built in each domain. It is convenient to use Parzen classifier with Gaussian kernel in the spatial domain due to its efficient implementation by convolution. The selection of spectral classifier depends on the actual segmentation problem. We have used a nearest mean classifier in the spectral domain. Results from both domains are put together by combining corresponding classifiers. The combined a posteriori probability then defines a new image labeling. The presented segmentation algorithm is an iterative procedure finished when no single pixel changes its label between subsequent iterations.

The algorithm has been developed in order to segment multi-spectral images of multi-component granules (e.g. laundry detergent powders) obtained by the method of SEM and energy-dispersive X-ray microanalysis (SEM/EDX). Several experiments on a set of five multi-spectral images have been performed. In our application, the number of classes is determined by the purpose of the analysis and by the structural properties of the powder specimen. It was, therefore, chosen a priori by the application expert. If automatic determination of the cluster count is of interest, some of methods, proposed in the literature, may be plugged in the initial clustering step.

In order to evaluate the performance of segmentation algorithms on this clustering problem, ground-truth was created manually by the application experts.

Probabilistic relaxation is another approach combining spectral and spatial information. We have built a probabilistic relaxation model, comparable to the setup of the presented algorithm and studied performance of both methods. The main difference between them is in the treatment of available data domains. The relaxation technique operates on the spectral information in the local neighborhood and its assumption of domain independence implies the use of the product combination rule. The classifier-based algorithm, on the other hand, completely separates the processing of the spatial and spectral domains and combines the outcomes in a general way.

It follows from our experiments, that the classifier-based segmentation method performed better than the consider relaxation model on our dataset. Although both algorithms provide a stable solution and their speed is comparable, relaxation method labeled several images erroneously. It also includes additional artifacts to the particle borders, which is a serious flaw in the considered application. The classifier-based segmentation method appears to provide satisfactory results, resembling the expert-made hand-labeling.

We have also investigated the use of a priori information for the segmentation of more images with similar spectral properties. A trained spectral classifier, which is a byproduct of the classifier-based algorithm, considerably speeds up the initial labeling step.

The use of the presented segmentation algorithm is not limited to the analysis of multi-component granules. It is a rather general approach for the combination of spatial and spectral (feature) information in image segmentation. The algorithm may be, therefore, applied to different types of multi-band images, as long as appropriate models are chosen for spectral and spatial classifiers. In presented application, images are generated pixel by pixel by an active scanner which produces high amount of noise compared e.g. to images acquired by CCD sensors. This noisy data is successfully modeled by linear or quadratic classifiers. Different types of data such as color images may require more sophisticated models reflecting complex non-linear structures in a spectral feature space. Future research will aim at the automatic determination of the number of classes (clusters) in the multi-spectral image of laundry detergents. A possibility of further splitting of classes by hierarchical clustering will be also investigated.

Acknowledgements

We would like to thank here P. Nootenboom for the acquiring of multi-spectral images used in experiments and D.M.J. Tax for fruitful discussions and comments on the manuscript.

References

[1] W.J. Christmas, J. Kittler, M. Petrou, Structural matching in computer vision using probabilistic relaxation, IEEE Trans. Pattern Anal. Mach. Intell. 18 (8) (1995) 749–764.

[2] R.P.W. Duin, D.M.J. Tax, Classifier conditional posterior probabilities, in: A. Amin, D. Dori, P. Pudil, H. Freeman (Eds.), Advances in Pattern Recognition, Lecture Notes in Computer Science, vol. 1451, Springer, Berlin, 1998, pp. 611–619, Proc. Joint IAPR Int. Workshops SSPR'98 and SPR'98, Sydney, Australia.

[3] J. Eklundh, H. Yamamoto, A. Rosenfeld, A relaxation method for multispectral pixel classification, IEEE Trans. Pattern Anal. Mach. Intell. 2 (1) (1980) 72–75.

[4] K. Fu, J. Mui, A survey on image segmentation, Pattern Recogn. 13 (1981) 3–16.

[5] J. Goldstein, D. Newbury, P. Echlin, D. Joy, A. Romig, C. Lyman, C. Fiori, E. Lifshin, Scanning Electron Microscopy and X-ray Microanalysis, Plenum Press, New York, 1992.

[6] R. Haralick, L. Shapiro, Survey: image segmentation techniques, CVGIP 29 (1985) 100–132.

[7] M. Hauta-Kasari, J. Parkkinen, T. Jaaskelainen, R. Lenz, Multispectral texture segmentation based on the spectral cooccurrence matrix, Pattern Anal. Appl. 2 (1999) 275–284.

[8] J. Hsiao, A. Sawchuk, Supervised textured image segmentation using feature smoothing and probabilistic relaxation techniques, IEEE Trans. Pattern Anal. Mach. Intell. 11 (12) (1989) 1279–1292.

[9] T. Huntsberger, C. Jacobs, R. Cannon, Iterative fuzzy image segmentation, Pattern Recogn. 18 (2) (1985) 131–138.

[10] M. Ismail, M. Kamel, Multidimensional data clustering utilizing hybrid search strategies, Pattern Recogn. 22 (1989) 75–89.

[11] J. Kittler, M. Hatef, R.P.W. Duin, J. Matas, On combining classifiers, IEEE Trans. Pattern Anal. Mach. Intell. 20 (3) (1998) 226–239.

[12] P. Lambert, L. Macairne, Filtering and segmentation: the specifity of color images, Int. Conf. Color Graph. Image Process. CGIP'2000 (2000).

[13] J. Matas, J. Kittler, Spatial and feature based clustering: applications in image analysis, Proc. CIAP95, Prague (1995) 162–173.

[14] P. Paclík, R.P. Duin, G.M. van Kempen, Multi-spectral image segmentation algorithm combining spatial and spectral information, Proc. SCIA 2001 Conf. (2001) (2001) 230–235.

[15] N.R. Pal, S.K. Pal, A reviewof image segmentation techniques, Pattern Recogn. 26 (9) (1993) 1277–1294.

[16] W. Skarbek, A. Koschan, Colour image segmentation—a survey. Technical report. Institute for Technical Informatics, Technical University of Berlin, October 1994, http://citeseer.nj.nec.com/skarbek94colour.html.

[17] M. Spann, R. Wilson, A quad-tree approach to image segmentation which combines statistical and spatial information, Pattern Recogn. 18 (3/4) (1985) 257–269.

[18] A. Stoddart, M. Petrou, J. Kittler, On the foundations of probabilistic relaxation with product support, J. Math. Imaging Vis. 9 (1998) 29–48.